Electronic Supplementary Information for

Direct Photoelectrochemical Oxidation of Hydroxymethylfurfural

Charles R. Lhermitte, Nukorn Plainpan, Pamela Canjura, Florent Boudoire, Kevin Sivula*

LIMNO, Ecole Polytechnique Fédérale de Lausanne, Lausanne, Switzerland

*kevin.sivula@epfl.ch

Experimental Details:

Synthesis of WO_3 electrodes on FTO coated glass

WO_3 electrodes were synthesized using a previously reported sol-gel deposition method.[S1,S2] To prepare the electrodes, 10 mmol (3.29 g) of sodium tungstate dihydrate was dissolved in 20 mL deionized water and run through a Dowex ion exchange column that had been acidified previously with 6 M HCl and rinsed back to pH 7 with Milli-Q water. A yellow solution was eluted into in a round-bottom flask containing 20 mL absolute ethanol while stirring. The resulting transparent yellow solution (tungstic acid) was concentrated on a rotary evaporator until the final volume was approximately 20 mL, at which time 6.6 g PEG-300 (TCI, lot. UP2XKAA, d 1.13) was added as a stabilizer. At this point, the solution was significantly more viscous and had a cloudy yellowish colour. The suspension was kept stirring constantly at 1200 rpm on a stir plate and used for up to 3 days. Over time the solution's colour turned dark green. However, this colour change did not appear to affect the consistency or quality of the resulting electrodes. WO_3 electrodes were synthesized by dropping 190 µL of the suspension onto clean 2.5 x 2.5 cm^2 FTO glass substrate (Solaronix) and spinning at 2500 rpm using a Laurel spin coater (Model WS-650MZ-23NPPB) for 30 seconds, followed by annealing the electrodes in a muffle furnace preheated to 500 °C for 30 minutes in air. A small section at the bottom of the electrode was masked with electrical tape to allow for an electrical contact. The spinning and annealing process was repeated ten times to obtain electrodes of sufficient thickness (ca. 2 µm).

Synthesis of $BiVO_4$ electrodes on FTO glass

$BiVO_4$ electrodes were prepared using our previously reported spin coating technique.[S3] Thin films of $BiVO_4$ were prepared by annealing a spin-coated solution of EDTA–metal complexes. To prepare the precursor solution, EDTA (36.53 g, 2 eq.) was added to 18.2 MΩ resistance water (100 mL, Millipore). A small amount of NH_4OH (12.5 mL) was added to partially deprotonate the EDTA, and ensure its dissolution. After the EDTA had dissolved, $Bi(NO_3)_3{\cdot}5H_2O$ (30.316 g, 1 eq.) was added. Upon contact with the solution, the solid formed a white cake, which slowly dissolved over time. Once the solid had completely dissolved, VO(AcAc) (16.57 g, 1 eq.) was added. To aid the dissolution of the blue powder, additional water was added, and the solution was heated to 60°C and left to stir for 1 h. After the solid had completely dissolved, the solution was left to cool. Once at room temperature, the pH

was measured and adjusted to 5, if necessary, by using dilute HNO_3 or NH_4OH. The final volume was adjusted to 250 mL by adding more water. The final concentrations of Bi, V, and EDTA were 0.25m, 0.25 m, and 0.5m, respectively.

$BiVO_4$ thin films were synthesized by spin coating the previously precursor solution. The spin coating was accomplished using a Laurell model WS-650MZ-23NPPB spin coater. For this, the substrate was first spun at 4500 RPMs, then 0.75 mL of the solution was dispensed on top. The electrode was kept spinning for 45 s after the solution was dispensed. Following the spin coating, the electrodes were calcined at 400°C in an air atmosphere to burn off all the organic material. After repeating the spin-coating/calcining cycles enough times to obtain electrodes of the desired thickness, the electrodes were annealed at 550°C for 1 h.

Synthesis of Fe_2O_3

Hematite thin films were prepared using a previously reported hydrothermal/annealing technique.[S4] Fluorine doped tin oxide (FTO)coated glass substrates (Solaronix TCO10-10, 8 Ω/sq.) were vertically positioned in a sealed glass bottle containing 1M sodium nitrate ($NaNO_3$, 99+ %, Acros) and 0.15M iron chloride hexahydrate ($FeCl_3 \cdot 6\ H_2O$, 99+ %, Acros) aqueous solution. The glass bottle was placed in an oven (Memmert UF 30 plus) for 3h at 100°C. During the heating process, β-FeOOH nanorods formed on the FTO surface. After the heating the β-FeOOH films were rinsed with high purity water (18.2 MΩ cm, Synergy), and finally they were annealed in a preheated tube furnace (MTI OTF-1200X-S) at 800°C for 15 min to convert the β-FeOOH to Fe_2O_3.

Synthesis of WO_3 thin films on Pt disk electrodes (for rotating disk electrode measurement)

Dense thin films of WO_3 were prepared on Pt disks using spray pyrolysis. For this, a precursor solution containing 0.1 M ammonium metatungstate and 1.1 g/100 mL PEG-300 was prepared using Millipore water. The prepared solution was sprayed onto a heated substrate using a custom-built spray pyrolysis apparatus. The substrate was heated to 500°C, and the solution was sprayed through a custom glass nozzle in pulses using compressed air as the carrier gas. For the pulsing, the solution was spayed for 5s, followed by 1s off. In between the solution spraying and the pause a cleaning delay of 3s was implemented. For the cleaning delay, the gas would flow through the nozzle, but the solutions would no longer be actively sprayed. This cleaning delay was necessary to avoid large droplets from accumulating at the tip of the nozzle. After the spray deposition process, the electrodes were calcined at 400°C under an air atmosphere to burn off the organic residues left behind from the PEG-300.

Preparation of Electrolyte solutions

0.1 M NaPi solutions were prepared by weighing 9.8 g of H_3PO_4 in a 2L beaker. The acid was then diluted to a volume of 1,000 mL by slowly adding Millipore water (18 MΩ cm). The solution pH was then adjusted to 4 using a pH meter and adding in a concentrated solution of NaOH.

Standard Electrochemical Measurements

All electrochemical measurements were collected using a BioLogic SP-200 potentiostat in a three-electrode configuration. Unless noted otherwise, the working, counter, and reference electrodes were WO_3, a Pt wire, and Ag/AgCl in saturated KCl. A buffered aqueous solution of 0.1 M NaPi at pH 4 was used as the electrolyte. All LSV experiments were performed at a scan rate of 20 mV/s. Unless noted otherwise, the illumination intensity was equivalent to 1 sun. The illumination direction for all experiments was from the back (glass) side.

Rotating ring disk electrode experiments

The rotating disk electrode measurements were performed using a RRDE-3a model rotating ring disk apparatus by ALS Co. supplied by CH instruments. The disk electrode mount housed a removable Pt disk onto which a dense, thick layer (c.a. 2.67 ±0.017 µm, see Fig. S1, ESI) of WO_3 was grown using spray pyrolysis, which prevents the Pt electrode underneath to be exposed to the electrolyte. The secondary working electrode was a platinum ring, the reference was Ag/AgCl (sat'd KCl), and the counter electrode was a platinum wire. Figure 1d (main text) depicts the results of the rotating ring disk photoelectrode experiments (RRDPE). For these experiments we used a 400 W xenon arc lamp with no filters. This was used in order to maximize the net current measured since the disk area was small (d = 4 mm, A = 12.56 mm^2). By applying a bias of 0.63 V vs. RHE, we determined that we should be able to observe the reduction of any O_2 that is formed at the disk. We expected that if O_2 was produced photoelectrochemically at the disk during a chopped light experiment, then we would observe a square wave reductive current response at the ring due to the reduction of O_2 to H_2O. Furthermore, when performing chronoamperometry under intermittent illumination, we observe no significant background current in the dark which would arise from Pt performing OER.

In the absence of HMF, we observe a small reductive ring current that we attribute to O_2 reduction. We note that the ring current is rather small, relative to the disk current. However, WO_3 is notoriously bad at performing OER. Previous reports indicate that WO_3 primarily produces H_2O_2 instead of O_2, and it also preferentially oxidizes anions that are present in the electrolyte. This behaviour has been reported previously in the literature by multiple groups, and would explain why small amounts of O_2 would be detected in the RRDPE measurment.[S1,S5-S7] Furthermore, we attempted to estimate the Faradaic efficiency from the RRDPE experiments, unfortunately, measuring a precise empirical collection efficiency for this apparatus was difficult, and the numbers we determined were unreliable. However, we consistently observed a negative ring current when operating the WO_3 disk electrode in pH 4 NaPi solution, which provides qualitative evidence that O_2 was formed under operation.

When 5 mM HMF is added to the solution, the ring current behaviour changes completely. After HMF is added, we observe a complete quenching of the reductive ring current signal. This result suggests that when HMF is added to solution, the OER is

effectively suppressed. This demonstrates that WO_3 will react preferentially with HMF, with little to no side reaction with H_2O to form O_2, even in aqueous solutions.

Extended-duration photo-oxidation experiments

Bulk-electrolysis experiments were performed in a custom-built two-sided cell (3D printed from Polyethylene terephthalate). The cell was composed of two compartments, which were separated by a Nafion membrane (N-115 membrane, 0.125mm thick). The membrane was required to prevent the diffusion of oxidised products to the counter electrode, where they could be reduced. The WO_3 photoelectrode, and Ag/AgCl reference electrode were contained in the working electrode compartment. The Pt wire was kept in the counter electrode compartment. The electrolyte solution used was 100 mL of 5 mM HMF in 0.1 M NaPi buffer, for the working electrode compartment, and 0.1 M NaPi buffer for the counter electrode compartment (also 100 mL). To eliminate potential diffusion limitations, the solution was kept stirring throughout the experiment using a magnetic stir bar. For the bulk electrolysis experiment, the current produced by the WO_3 photoelectrode was measured over 64 hours at an applied potential of 0.683 V vs. RHE. The illumination intensity used was equivalent to 3 suns, and the electrodes were illuminated from the back (glass) side. The active area of the WO_3 photoelectrode was ca. 2.5 cm^2. Three runs of 64 h were completed and the data averaged.

Oxidation products quantification

Product quantification during the bulk electrolysis experiment was performed using an HPLC coupled to a UV-Vis spectrometer (Shimadzu Prominence LC-20AP HPLC, equipped with dual UV-Vis detector set at 255 and 285 nm). 600 µL aliquots were taken before, during and after the photo-oxidation experiment. Sulfuric acid (5 mM) was used as the mobile phase in the isocratic mode. An equilibration time of 30 minutes was required before the first injection. The flow rate was 0.5 mL min^{-1} at 40 ˚C. The samples were injected through polytetrafluoroethylene hydrophilic filter (0.22 µM pore size) into a Coregel 87H3 7.8 × 300 mm column (part number CON-ICE-99-9861) that was purchased from BGB Analytik AG in Switzerland. The product identification and quantification were determined from calibration curves from the known standards. The retention times for HMF, DFF, HMFCA, FFCA and FDCA were 42.2, 53.2, 27.7, 29.6 and 21.1 minutes respectively.

Microscopy, XRD and Raman Spectroscopy

SEM data was collected using a Zeiss Gemini 300 scanning electron microscope in HV mode. XRD data was collected using a Panalytical Empyrean system (Theta-Theta, 240mm) equipped with a PIXcel-1D detector, Bragg-Brentano beam optics (including hybrid monochromator) and parallel beam optics. Raman spectra were obtained with a LabRam spectrometer (Jobin Yvon Horiba). The excitation line was provided by an Ar laser (532.19 nm).

Materials

The following chemicals were used as received without further purification. HMF (99%), DFF (97%), and ammonium meta tungstate were purchased from Sigma-Aldrich. $NaWO_4$ (99%) and Dowex® 50WX2, 100-200 mesh were purchased from Acros Organics. HMFCA was obtained from Apollo Scientific. Nafion® membrane was obtained from Alfa Aesar. FFCA (95%) was purchased from ABCR. FDCA (97%) was purchased from fluorochem.

Chemical Kinetic model and rate constant fit

The kinetic modelling and fitting were performed using a custom Python script. The source code is hosted on Github: https://github.com/flboudoire/chemical-kinetics and its documentation can be found here: https://chemical-kinetics.readthedocs.io/en/latest. Firstly, it was necessary to make a few approximations. We suppose that all the reactions presented are pseudo first order. Davis and co-workers have demonstrated that this is a reasonable assumption[S1] In their work, they studied the mechanism of HMF oxidation and demonstrated that it proceeds through oxidations at the alcohol and aldehyde moieties, which are first order reactions. Additionally, we assumed that the reductive reverse reactions are negligible since we are operating at a high forward bias. Due to the presence of a significant electric field at the electrode surface, the WO_3 surface will be depleted of electrons, and thus little to no reductive currents due to the reverse reaction will be possible under these conditions. According to the law of mass action the rates of concentration change for the reaction of a species A at the photoelectrode surface with two holes at the WO_3 / electrolyte interface to give a product B can be written, in general, as follows:

$$\frac{d[A]_{surf}}{dt} = -k[h]^2[A]_{surf} \quad \text{(S1)}$$

$$\frac{d[B]_{surf}}{dt} = k[h]^2[A]_{surf} \quad \text{(S2)}$$

Where $[A]_{surf}$ and $[B]_{surf}$ are the concentrations of A and B in the electrolyte at the surface of WO_3, [h] is the concentration (activity) of holes available at the surface, and k is the (true) reaction rate constant. To simplify these equations, we consider that the reactions are under kinetic control and the hole concentration at the surface is in excess and therefore can be considered constant. This is justified by the fact that we operate at a potential where the photocurrent for HMF oxidation is close to saturation (see Figure S4). We also measured a significant drop in photocurrent if the solution was not stirred (see Figure S5), further proving that the reactions not limited by [h] but rather the concentration of the molecular reactant at the surface.

We also consider that the species concentrations measured in the bulk of the solution change in the same proportion as the species concentration at the surface of the electrode. This hypothesis is supported by their similar molecular size, hence reasonably similar and constant mass transfer coefficients, k_m. Considering these

hypotheses, equations (S1) and (S2) can be rewritten with $k' \approx k[h]^2$, and $[A]_{surf} \approx (k_m/(1+k_m))\,[A]_{solution}$ as follows:

$$\frac{d[A]_{solution}}{dt} = -k'[A]_{solution} \quad (S3)$$

$$\frac{d[B]_{solution}}{dt} = k'[A]_{solution} \quad (S4)$$

In this case, considering the reactions proposed in Figure 2c, the system of differential equations that model the concentrations measured in solution (Figure 2b) are written as follows:

$$\frac{d[HMF]}{dt} = -(k_{11}+k_{12}+k_{B1})[HMF] \quad (S5)$$

$$\frac{d[DFF]}{dt} = k_{11}[HMF] - (k_{21}+k_{B21})[DFF] \quad (S6)$$

$$\frac{d[HMFCA]}{dt} = k_{12}[HMF] - (k_{22}+k_{B22})[HMFCA] \quad (S7)$$

$$\frac{d[FFCA]}{dt} = k_{21}[DFF] + k_{22}[HMFCA] - (k_3+k_{B3})[FFCA] \quad (S8)$$

$$\frac{d[FDCA]}{dt} = k_3[FFCA] - k_{B4}[FDCA] \quad (S9)$$

$$\frac{d[B]}{dt} = k_{B1}[HMF] + k_{B21}[DFF] + k_{B22}[HMFCA] + k_{B3}[FFCA] + k_{B4}[FDCA] - k_B[B] \quad (S10)$$

$$\frac{d[B^*]}{dt} = k_B[B] \quad (S11)$$

With this model, we can extract quantitative reaction rate constants for all the intermediate reactions leading to the formation of FDCA. We can also characterize the speculated formation of oxidized by-products (B) and their further oxidation to B*. We also simultaneously model the amount of charge passed during the course of the reaction (Figure 2a, main text). This current data represents a sum of contributions from all species formed during the photoelectrochemical oxidation of HMF. Since our RRDE data demonstrates that OER is not a significant competing reaction (Figure 1d, main text), we are able to safely make this assumption. The following equation is used to model the evolution of passed charge over time:

$$Q = qN_AV\sum_i n_iC_i \quad (S12)$$

With Q being the total amount of charge passed, q the electron charge (1.6×10^{-19} C), N_A Avogadro's number (6.02×10^{23}), V the volume of solution (100 mL in our case), n_i the amount of charge passed to make one molecule of species i, and C_i is the concentration of species i. Numerically solving the set of differential equations (Equations (S5)-(S11)) and using a least-square fit algorithm with the experimental data, the numerical solution, and Equation S12 we can extract a set of eleven rate

constants that fit the behaviour observed in Figure 2a and b. The main discrepancy is in the predicted DFF concentration over time for our model, which underestimates the experimental value. This suggests that our model slightly underestimates the value of k_{11}.

Supplementary Figures and Tables.

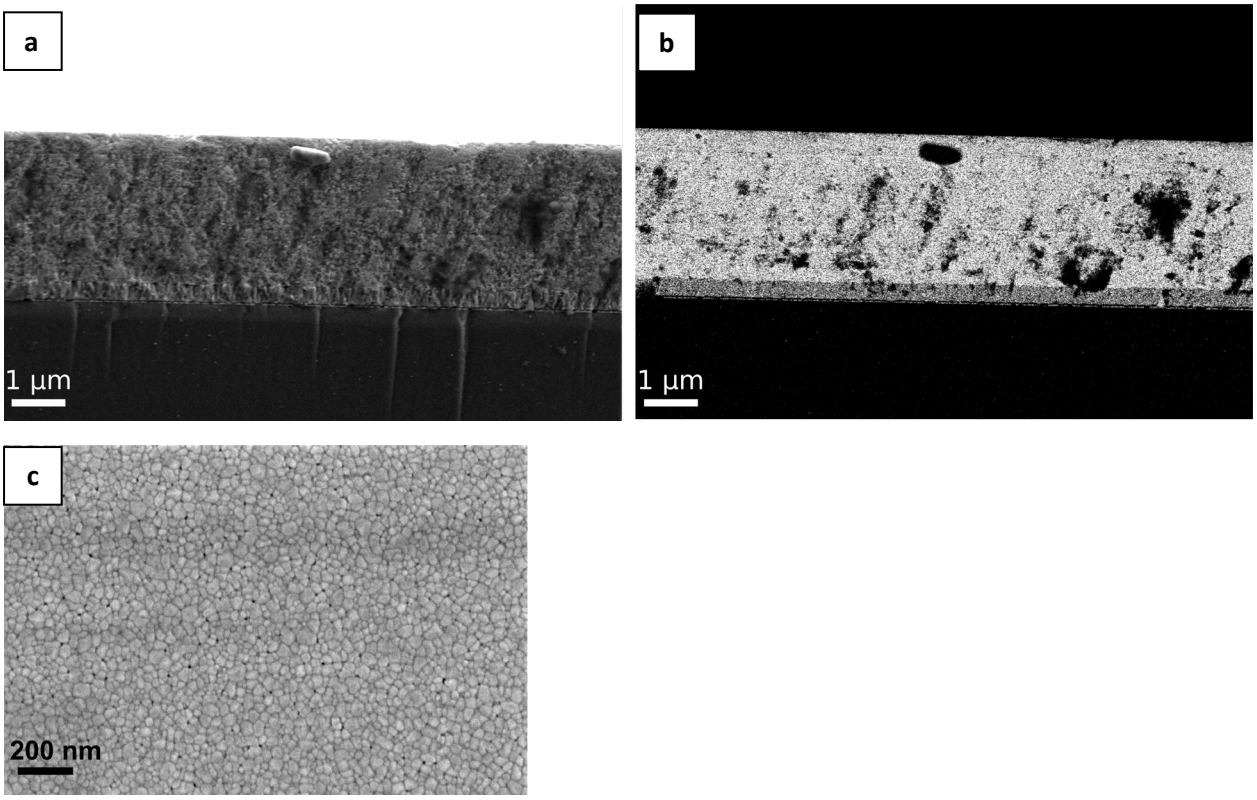

Fig S1. WO3 films used for RRDE (a,b) cross sectional SEM images of a WO_3 thin film grown via spray pyrolysis on an FTO coated glass substrate. (a) was collected using the standard secondary electron detector, and b was obtained using the backscattered electron detector in order to obtain better contrast between the FTO and WO_3 thin films. Cross sectional images demonstrating clearly the film thickness on the Pt substrate were difficult to obtain since the WO_3 thin film curled over the edge of the substrate. (c) depicts a top down image of WO_3 grown onto a Pt disk electrode. We note that no exposed Pt was observed, so we expect little to no current response from the underlying Pt substrate in our RRDPE measurements.

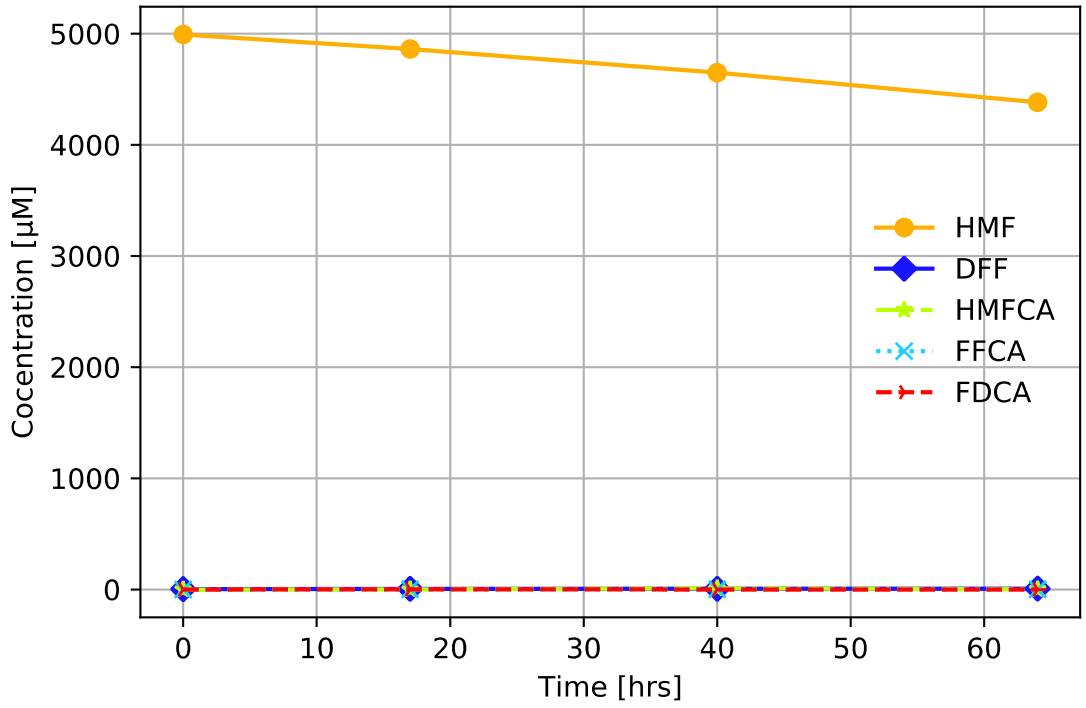

Figure S2. Concentration of HMF, DFF, FFCA, HMFCA, and FDCA over time. For this experiment a 5 mM solution of HMF in 0.1M pH 4 KPi was irradiated with simulated 3 Suns. The species concentration over time was monitored using and HPLC coupled to a UV-Vis.

Table S1. Concentration of HMF, DFF, FFCA, HMFCA, and FDCA over time of the control experiment (Figure S2).

	Concentration [µM]			
Compound	**0 h**	**17 h**	**40 h**	**64 h**
HMF	4992	4861	4649	4382
DFF	3	6	6	8
HMFCA	0	1	0	2
FFCA	0	1	0	1
FDCA	0	0	0	0

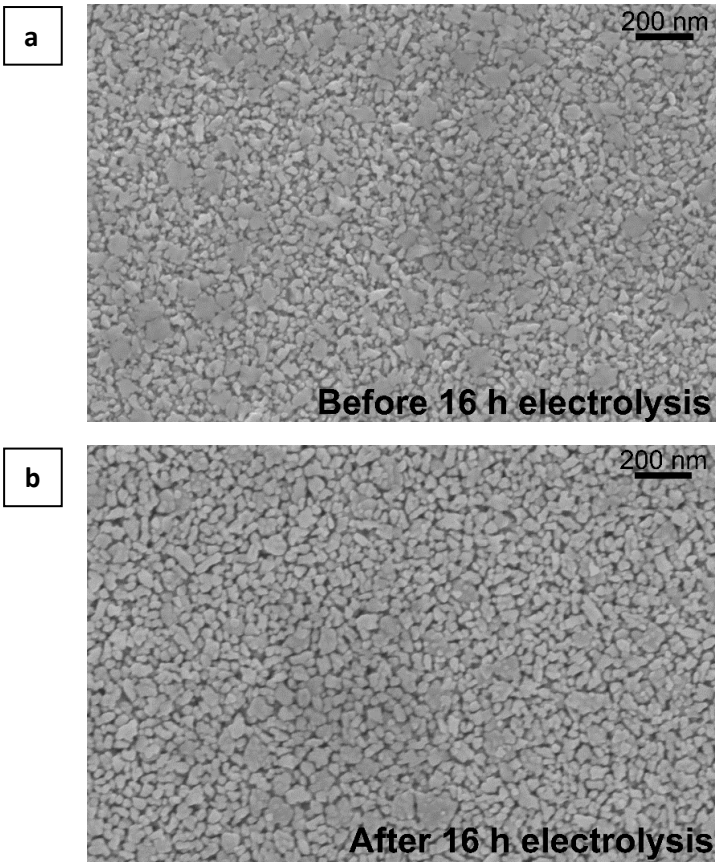

Figure S3. SEM images of a WO_3 electrode (a) before, and (b) after a 16 h bulk electrolysis experiment. This time frame was selected since it was after the largest observed photocurrent decrease. The bulk electrolysis experiment was performed at 0.683 V vs. RHE under simulated 3 suns illumination in a pH 4 0.1M KPi solution which contained 5 mM HMF.

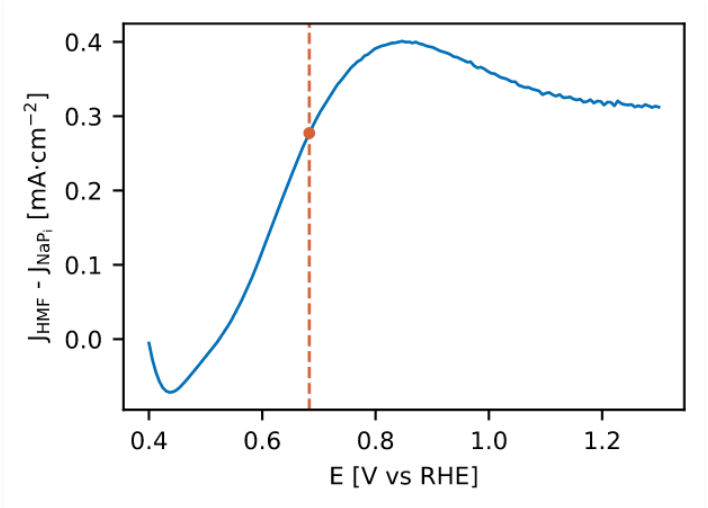

Figure S4. Difference between the LSV with and without HMF under 3 suns in pH 4 KPi solution. The vertical line depicts the photocurrent density at the applied bias used in the bulk electrolysis experiments. See section "Chemical Kinetic model and rate constant fit" in the ESI for more information.

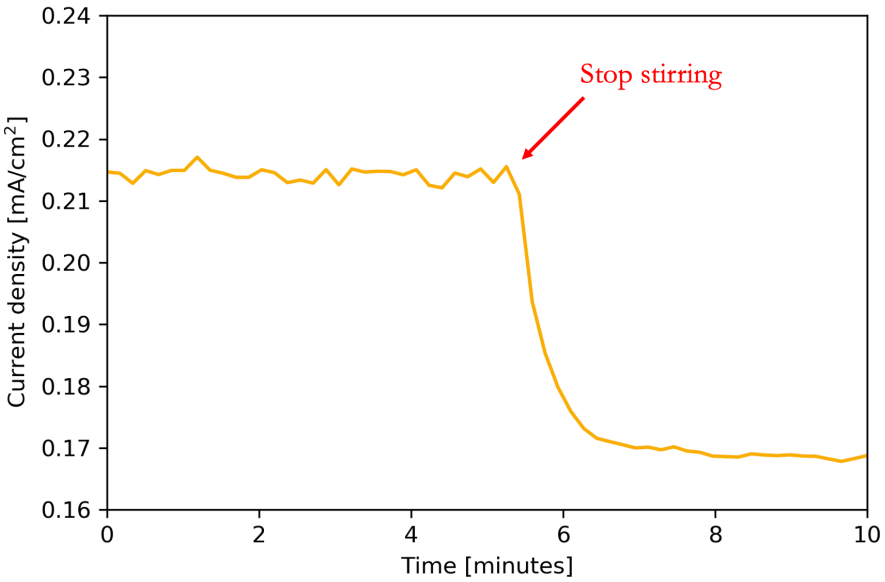

Figure S5. Chronoamperometry of HMF oxidation on WO_3 under simulated 3 suns in pH 4 KPi solution showing the impact of stirring the solution on the photocurrent. See section "Chemical Kinetic model and rate constant fit" in the ESI for more information.

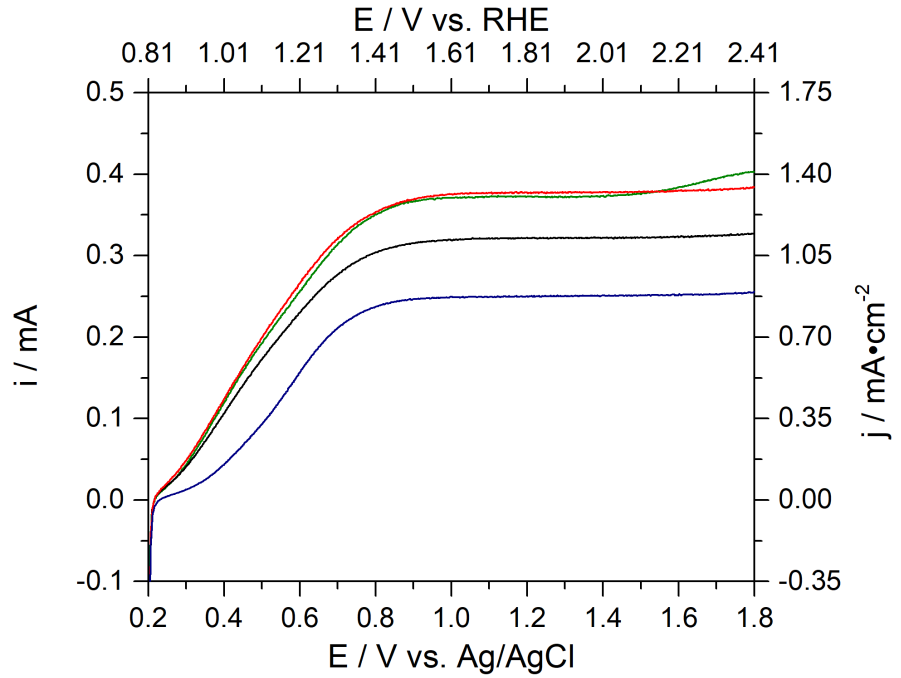

Figure S6. LSVs of WO_3 electrodes under simulated 1 sun illumination in solutions containing 5mM HMF (red), 5mM DFF (black), 5mM BHMF (olive), and a blank control solution (navy). All solutions were prepared using 0.1 M NaPi buffered to pH 4.

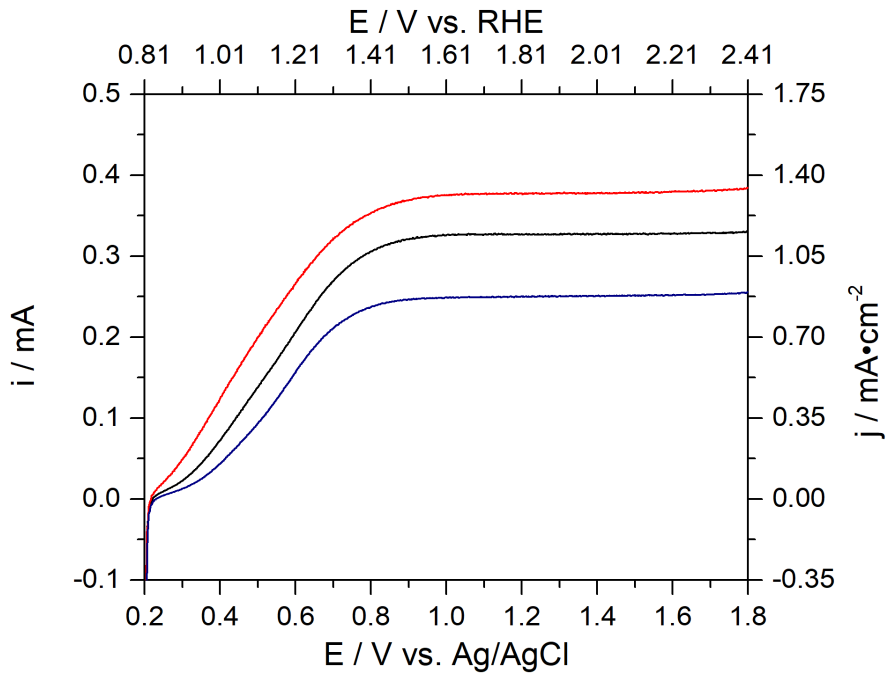

Figure S7. LSVs of WO_3 electrodes under simulated 1 sun illumination in solutions containing 5mM HMF (red), 5mM FDCA (black), and a blank control solution (navy). All solutions were prepared using 0.1 M NaPi buffered to pH 4.

Supplementary References

S1. Lhermitte, C. R., Verwer, J. G. & Bartlett, B. M. Improving the stability and selectivity for the oxygen-evolution reaction on semiconducting WO_3 photoelectrodes with a solid-state FeOOH catalyst. *Journal of Materials Chemistry A* **4**, 2960–2968 (2016).

S2. Santato, C., Odziemkowski, M., Ulmann, M. & Augustynski, J. Crystallographically Oriented Mesoporous WO3 Films: Synthesis, Characterization, and Applications. *J. Am. Chem. Soc.* **123**, 10639–10649 (2001).

S3. Lhermitte, C. *et al.* Generalized Synthesis to Produce Transparent Thin films of Ternary Metal Oxide Photoelectrodes. *ChemSusChem* **n/a**, (2020).

S4. Liu, Y., Le Formal, F., Boudoire, F. & Guijarro, N. Hematite Photoanodes for Solar Water Splitting: A Detailed Spectroelectrochemical Analysis on the pH-Dependent Performance. *ACS Appl. Energy Mater.* **2**, 6825–6833 (2019).

S5. Mi, Q., Zhanaidarova, A., S. Brunschwig, B., B. Gray, H. & S. Lewis, N. A quantitative assessment of the competition between water and anion oxidation at WO_3 photoanodes in acidic aqueous electrolytes. *Energy & Environmental Science* **5**, 5694–5700 (2012).

S6. Hill, J. C. & Choi, K.-S. Effect of Electrolytes on the Selectivity and Stability of n-type WO_3 Photoelectrodes for Use in Solar Water Oxidation. *The Journal of Physical Chemistry C* **116**, 7612–7620 (2012).

S7. Davis, S. E., Zope, B. N. & Davis, R. J. On the mechanism of selective oxidation of 5-hydroxymethylfurfural to 2,5-furandicarboxylic acid over supported Pt and Au catalysts. *Green Chem.* **14**, 143–147 (2012).